



Machine Learning Approach in the Prediction of Fog: An Early Warning System

ANAND SHANKAR^{#*}, ASHISH KUMAR^{*} and VIVEK SINHA^{**}

[#]Department of Electronics & Communication Engineering, National Institute of Technology, Patna, India.

^{*}India Meteorological Department, Ministry of Earth Sciences, Govt. of India, Patna, India.

^{**}India Meteorological Department, Ministry of Earth Sciences, Govt. of India, New Delhi, India.

(Received 09 June 2022, Accepted 17 June 2024)

e mail: anands.ph21.ec@nitp.ac.in

सार-विमानन क्षेत्र कोहरे के प्रति बेहद संवेदनशील है। इसलिए, विमानन क्षेत्र की दक्षता, विशेष रूप से हवाई अड्डा प्रबंधन और उड़ान समय-निर्धारण के लिए सटीक कोहरे की पूर्वानुमान आवश्यक है। संख्यात्मक मौसम पूर्वानुमान मॉडल और मार्गदर्शक प्रणालियों के साथ भी कोहरे की पूर्वानुमान चुनौतीपूर्ण है। कोहरे के पूर्वानुमान की कठिनाई का कारण सूक्ष्म पैमाने के कारकों की समझ है जो सीमा परत में कोहरे के बनने, तीव्र होने, बढ़ने और फैलने का कारण बनते हैं। इस अध्ययन का उद्देश्य यह देखना है कि मशीन लर्निंग (ML) उपकरण भारत के इंडो-गांगेय के मैदानों (IGP) का एक प्रतिनिधि स्टेशन जय प्रकाश नारायण अंतर्राष्ट्रीय हवाई अड्डे (ICAO इंडेक्स-VEPT) पर कोहरे (दृश्यता <1000 मीटर) और घने कोहरे (दृश्यता <200 मीटर) का पूर्वानुमान कितनी सटीकता से कर सकते हैं। प्रस्तावित एनसेंबल ML-आधारित मॉडल को 2014 से 2020 तक प्रति घंटे के सिनॉप्टिक डेटा का उपयोग करके प्रशिक्षित किया गया और 2021 से 2022 (दिसंबर से फरवरी) तक के डेटा का उपयोग करके परीक्षण किया गया। एक बार जब विशेषताएं चुन ली जाती हैं और पूर्वानुमानकर्ताओं के स्थानीय ज्ञान को ध्यान में रखा जाता है, तो प्रस्तावित ML मॉडल बनाने के लिए शुष्क बल्ब तापमान (डिग्री सेल्सियस), ओस बिंदु तापमान (डिग्री सेल्सियस), सापेक्ष आर्द्रता (%), बादल की मात्रा (ऑक्टा), हवा की दिशा (सही उत्तर से डिग्री) और हवा की गति (नॉट्स) का उपयोग किया जाता है। 0000 UTC पर अगले दिन कोहरे (दृश्यता <1000 मीटर) और घने कोहरे (दृश्यता <200 मीटर) का पूर्वानुमान करने के लिए 1500 से 2200 UTC के मौसम संबंधी डेटा पर ML एल्गोरिदम को प्रशिक्षित किया गया, जिसमें दो घंटे का अग्रकाल था। 00 UTC पर 4 घंटे के अग्रकाल के साथ कोहरे के पूर्वानुमान के लिए, ML मॉडल को 13 से 20 UTC और इसी तरह के डेटा के साथ प्रशिक्षित किया गया। यह अध्ययन छह लेवल 0 ML मॉडल में प्राचल ट्यूनिंग का मूल्यांकन करता है: वितरित रैंडम फ़ॉरेस्ट (DFR), डीप लर्निंग (DL), ग्रेडिएंट बूस्टिंग मशीन (GBM), सामान्यीकृत रैखिक मॉडल (GLM), एक्सट्रीमली रैंडमाइज्ड ट्री (XRT), एक्सजीबूस्ट, और लेवल 1 पर स्टैकड एन्सेम्बल। प्रदर्शन मेट्रिक्स और सांख्यिकीय कौशल स्कोर संकेत देते हैं कि SRF और DL मॉडल कोहरे (दृश्यता <1000 मीटर) और घने कोहरे (दृश्यता <200 मीटर) के लिए लेवल 0 पर 2 और 4 घंटे के अग्रकाल के लिए अच्छा प्रदर्शन करते हैं। लेकिन प्रस्तावित एन्सेम्बल मॉडल लेवल 0 पर सभी बेस मॉडल से बेहतर प्रदर्शन करते हैं और पटना एयरपोर्ट पर कोहरे की पूर्वानुमान करने के लिए सबसे अच्छे उपकरण के रूप में पहचाने जाते हैं।

ABSTRACT. The aviation sector is extremely vulnerable to fog. Thus, accurate fog predictions are essential for aviation sector efficiency, particularly airport management and flight scheduling. Even with numerical weather prediction models and guiding systems, fog prediction is challenging. The difficulty of fog prediction is due to the inability to grasp the micro-scale factors that cause fog to form, intensify, augment and dissipate in the boundary layer. This study looks at how well machine learning (ML) tools can predict fog (Visibility <1000 m) and dense fog (Visibility <200 m) at India's Jay Prakash Narayan International Airport (ICAO Index-VEPT), a representative station of the Indo-Gangetic Plains (IGP). The proposed ensemble ML-based model was trained using hourly synoptic data from 2014 to 2020 and tested using data from 2021 to 2022 (December to February). Once the features are chosen and the forecasters' local knowledge is taken into account, the dry bulb temperature (°C), dew point temperature (°C), relative humidity (%), cloud amount (octa), wind direction (degrees from true north) and wind speed (knots) are used to build the proposed ML models. ML algorithms were trained on meteorological data from 1500 to 2200 UTC to predict fog (Visibility <1000 m) and dense fog (Visibility <200 m) for the next day at 0000 UTC, with a two-hour lead time. For fog forecasting at 0000 UTC with a

4-hour lead time, ML models were trained with data from 1300 to 2000 UTC and so on. This study evaluates parameter tuning in six level 0 ML models: distributed random forest (DFR), deep learning (DL), gradient boosting machine (GBM), generalized linear model (GLM), extremely randomized tree (XRT), XG Boost and stacked ensemble at level 1. The performance metrics and statistical skill scores indicate that DRF and DL models perform well for lead times of 2 and 4 hours at level 0 for fog (visibility <1000 m) and dense fog (visibility <200 m). But the proposed ensemble models outperform all the base models at level 0 and are recognized as the best instrument for predicting fog at Patna Airport.

Key words - Fog prediction, Machine learning algorithms, Indo-Gangetic plains, Ensembling, Aviation services.

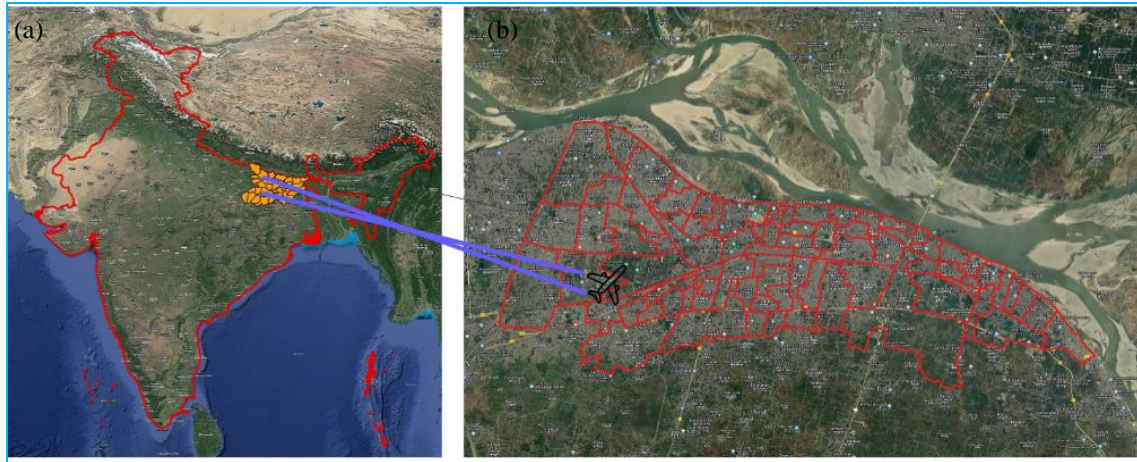
1. Introduction

Fog is a suspension of microscopic water or ice droplets that reduces horizontal visibility on Earth to less than one kilometer (World Meteorological Organization 2018, 2019). Another local setting of the fog indicator is relative humidity, which should be 90% or above (IMD, Ministry of Earth Sciences, 2021). Fog forms when surface temperatures are low, the wind is light, and atmospheric conditions are stable, chilling the surface layer to near saturation. Other than radiation fog, which forms in situ, advection fog can grow on a huge landmass and travel to neighboring locations as the wind blows. In the Indo-Gangetic Plains (IGP) regions, the three months of the year, namely December, January and February, are noted for intense fog spells. Therefore, most of the economic losses and mishaps because of low visibility usually occur in only these three months. Large-scale fog hampers surface, rail and air transportation, causing economic loss. Recent fog research in India found worrying increases in fog and land pollution in these specific months in the IGP, causing socio-economic issues (Tyagi *et al.*, 2017). Dense fog causes aircraft delays, cancellations, and diversion at airports (Mitsokapas *et al.*, 2021), suffering passengers and costing airlines money (Shankar and Giri, 2024). Low visibility of less than 800 metres impairs takeoff and landing at major airports in this region (Hosea, 2019). Modern airports feature an ILS, but pilots still need a visual reference to land. Low visibility can severely impair air navigation. The proposed study uses ensemble ML approaches to predict fog (visibility <1000 m) and dense fog (visibility <200 m) at 0000 UTC at Patna airport. The 2014-22 datasets of the foggy seasons in the IGP regions (December to February) were used to train and test the ML-based ensemble model. For proper evaluation and ML model parameter adjustment, the statistical characterization of Patna Airport fog is also looked into. The study yielded encouraging results that could benefit aviation services by tapping the potential of an ensemble of ML approaches. The paper is organized as follows: The related works are presented in Section 2, the explanation of the study areas and datasets presented in Section 3, the detailed methodology discussed in Section 4, the results in Section 5, and the discussion and definitive conclusion presented in Sections 6 and 7, respectively.

2. Related works

Most studies on fog have used statistics to describe its short- and long-term persistence (Belo-Pereira and Santos, 2016; Cornejo-Bueno *et al.*, 2020; Salcedo-Sanz *et al.*, 2021), long- and short-term period (Izett *et al.*, 2019), onset (Steenefeld *et al.*, 2015; Kutty *et al.*, 2019), and dynamic process (Haeffelin *et al.*, 2013; Mazoyer *et al.*, 2017). Out of this, most of the studies are based on conventional regression methods with a limited success rate. With the help of local causative factors, data-driven ML approaches are showing increasing promise and have the potential to revolutionize visibility forecasting. In the last decade, ML techniques have been successfully applied to predict low visibility and fog-related extreme events in some countries (Boudala *et al.*, 2012; Jonnalagadda and Hashemi, 2020; Miao *et al.*, 2020). Neural networks (Colabone *et al.*, 2015), Bayesian decisions (Boneh *et al.*, 2015), support vector regression (Cornejo-Bueno *et al.*, 2017), Extreme Learning Machines (ELM) (Cornejo-Bueno *et al.*, 2021), and evolutionary neural approaches (Durán-Rosal *et al.*, 2018) are examples. Airport fog prediction is the focus of several of these earlier works. Other research examines fog's meteorological causes (Stolaki *et al.*, 2015; La *et al.*, 2020). Some studies are also using the Decision Tree algorithm to forecast fog using NWP model output weather data (Bartoková *et al.*, 2015) and synoptic weather observed data (Shatunova *et al.*, 2015). Table 1 lists the major contributions to fog prediction using ML approaches.

Despite many studies, understanding complex and chaotic atmospheric processes on a short time and domain scale remains one of the biggest challenges for location-specific fog (visibility) forecasts. The NWP model has only partially resolved several of these interconnected processes (Singh *et al.*, 2018; Pahlavan *et al.*, 2021) with limited success. In numerical weather-predicting models, fog prediction is sensitive to initial conditions; therefore, any error in the initial condition causes a large-scale difference between predicted and actual values. Even with these drawbacks, NWP multi-rule-based post-processing fog prediction is a promising method (Payra and Mohan, 2014). However, a machine learning-based prediction model uses its memory function to identify and match the



Figs. 1(a&b). The geographical location of Jay Prakash Narayan International Airport Patna(a) in India (b) and the capital cities of Patna and its airport.

TABLE 1

Important Works Related to the Prediction of Fog.

ML approaches in the prediction of fog	Contribution and differences with the previous approaches
Application of deep learning in airport visibility forecasting (Zhu <i>et al.</i> , 2017).	The neural network-based DNN technique is used to forecast the low-visibility range. The proposed model sometimes shows an error of more than 2000 m. However, the innovative deep learning used in visibility forecasting has great promise for the future.
Probabilistic Nowcasting of Low-Visibility Procedure States at Vienna International Airport During the cold season (Kneringer <i>et al.</i> , 2019).	The probabilistic forecasting technique is based on ordered logistic regression. Used the best viable resources to overcome the visibility of the airports, the accuracy and sensitivity of the models are limited.
Probabilistic Visibility Forecasting Using Bayesian Model Averaging (Boneh <i>et al.</i> , 2015)	The proposed model is based on the Bayesian decision network. Models show great promise but lack robustness in the model outcome.

current data set with historical data at multiple levels, making the prediction more objective and reducing the chance of erroneous data corrupting the process.

3. Study areas and dataset

3.1. Study areas

This study looks at synoptic weather observations made every hour at Patna's Jay Prakash Narayan International Airport (JPNI), which can be found at 25.5947° N, 85.0908° E (Fig. 1). The region surrounding the airport is susceptible to frequent occurrences of low-visibility events, which can be attributed to both local geographical characteristics and fog patterns associated with western disturbances (WD). Patna Airport is situated at a relatively low elevation of 52 metres within the

alluvial plains of the Ganga basin. From December to February, radiation fog and advection fog were common in this area because of the Western Disturbance (WD) (Badarinath *et al.*, 2009; Sawaisarje *et al.*, 2014). The occurrence of dense fog in this particular area often leads to the shutdown of airports or substantial delays, resulting in wide-ranging economic and social implications. Therefore, our research was centered on an airport located in the Indo-Gangetic Plain (IGP) region, which is known to frequently encounter foggy conditions (as depicted in Fig. 1).

3.2. Dataset

In this dataset, the moment (x_n) and the previous hours (x_{n-2} to x_{n-8}) are used to predict the target value in the hour (y_{n+2}) for a two-hour lead time, the hour (y_{n+4}) for

TABLE 2

The meteorological parameter of METAR (synoptic hours) is optimally used

Meteorological Parameter	Code	Type	Units
Wind Direction	ddd	Factor	°North
Wind Speed	ff	Factor	Knots
Dry Bulb Temperature	tt	Numeric	°C
Dew Point Temperature	td	Numeric	°C
Relative Humidity	rh	Numeric	%
Cloud Cover	n	Factor	octa

a four- hour lead time, and so on to predict fog or dense fog. ML algorithms to predict fog (surface visibility <1000 m) and dense fog (surface visibility <200 m) using hourly meteorological parameters such as dry bulb temperature dew point temperature, wind speed, wind direction, relative humidity, cloud amount, *etc.* (the details are presented in Table 2). These parameters were decided based on the feature selection as well as local knowledge of the onset and dissipation of fog and dense fog.

For reliable predictions, non-linear prediction models are better for this dataset since the specified input factors and the current value of the predictive variables (fog or dense fog) do not have a direct or linear relationship. The linear correlation between variables is only a suggestion and should be treated with caution due to the non-linear interactions between meteorological variables that generate fog episodes. This study used weather data from December, January and February of 2014-15 to 2020-21 (a total of 21 months) to train the models. It then used weather data from 2021-22 (3 months) to test the best machine learning (ML) approaches (level 0 and level 1). Fog/no fog ratios are 140/493 and 43/47 in the train and test datasets. In the train and test datasets, the dense fog/no dense fog ratios are 51/582 and 11/79.

4. Methodology

The core ideas that underlie all methodologies can be distilled into the notion of a dataset $(x, y)_{i=1}^N$, where $x = (x_1, \dots, x_d)$ denotes the input of descriptive variables & y represents the corresponding response variable label. The objective of these estimation approaches is to reconstruct the unknown functional relationship between x and y by means of estimating the value of $f(x)$. Consequently, the value of the loss function $\Psi(y, f)$ is minimized.

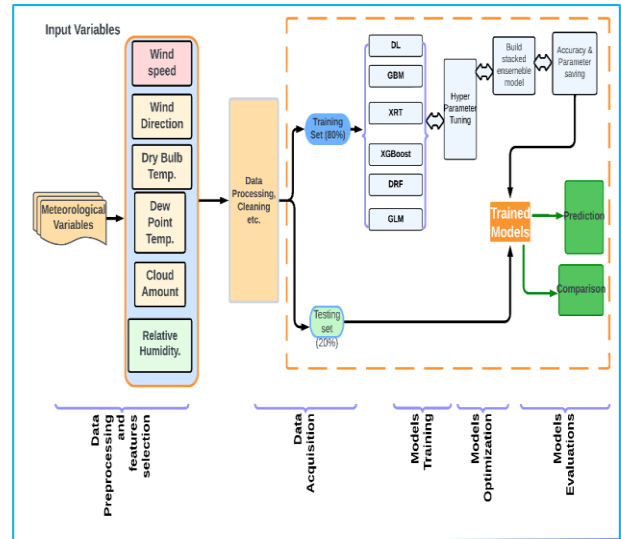


Fig. 2. Process block diagram of the proposed machine learning prediction model.

$$\widehat{f(x)} = y \quad (1)$$

$$\widehat{f(x)} = \arg \min_{f(x)} \Psi(y, f(x)) \quad (2)$$

Equation (1) represents the relationship between the function $f(x)$ and the variable y . Equation (2) denotes the argument that minimizes the function $f(x)$ with respect to the variables y and $f(x)$.

$$\widehat{f(x)} = \arg \min_{f(x)} \text{Ex}[Ey \Psi[y, f(x)] | x] \quad (3)$$

The expression in equation no. 3 demonstrates the relationship between the expected loss function and the change in the response variable, denoted as Ey ($\Psi[y, f(x)]$). This change is influenced by the observed descriptive data, represented by x . The selection of response y can be made from a distribution that exhibits skewness. There exist a multitude of loss functions that have the potential to impact this phenomenon. The consideration of binomial loss in classification issues becomes straightforward when the response variable exhibits dual variance, specifically when it takes on two distinct values ($y = 0, 1$). Fig. 2 illustrates a block schematic depicting the comprehensive process via which our suggested machine-learning prediction model functions. The detailed technique is elucidated in Algorithm 1, which is presented below. The algorithms described were built using the Python programming language with the assistance of the H₂O and Anaconda software platforms.

The details of the algorithms described in the methodology presented below

Algorithm-1: Proposed stacked ensemble approaches for the prediction of fog (surface visibility <1000 m) and dense fog (surface visibility <200 m) for the lead time of 04 hours and 02 hours
Input: $x(n)$ to $x_d(n)$: Previous 08 synoptic hour's datasets of the 06 weather parameter
Output: $y(n)$: Occurrence of fog (visibility <1000 m) or dense fog (visibility <200 m)
Procedure:
1) <i>Preprocess the datasets</i>
2) <i>Feature Selection using principal component analysis (PCA) Co-variance matrix method</i>
3) <i>Tuning of ML approves at level 0</i>
(a.)
I. GBM: Distribution: "bernoulli", ntrees=45, max_depth=6, min_rows=15, learn_rate=0.2, fold_assignment = "Modulo", keep_cross_validation_predictions = True.
II. DRF: ntrees =38, max_depth =20, min_rows = 10, keep_croo_validation = True, fold_assignment = "Modulo" , keep_cross_validation_predictions = True.
III. GLM : family = binomial, lambda = 0, compute_p_values = True
IV. XRT : histogram_type = (uniformadaptive), fold_assignment = " modulo", keep_cross_validation = True.
V. DL (Deep Learning): Distribution: Bernouli, hidden = 50, epochs = 3512 , train_samples_per_iteration = -2 , activation = "Rectifier With Dropout", score_training_samples = 10000
VI. XGBoost: n_estimators = 55, lambda = 1, gamma = 0, max_depth = 3.
(b) Ensembling of ML approaches at level 1 (of level 0)
Stacked Ensemble: Type : binomial ensemble , base_models =
([GBM , DRF , GLM , XRT , DL(deep learning) , XGBoost])
4) <i>Evaluate performance using $y(n)$ and $f(n)$:</i>
5) <i>Performance comparison of proposed method with various state-of-the-art methods in terms of performance indexes.</i>
6) <i>Output: $\{y_d(n), Performance indexes\}$</i>
End of procedure

4.1. Algorithms

4.1.1. Gradient Boosting Machine (GBM)

This forward-learning ensemble classification technique employs boosting to increase performance. A decision tree is fitted to the data first. After the first tree is evaluated, the second tree is built to cover the difference between it and the actual target (Elith *et al.*, 2008). The residue is rebuilt. When paired with the prior tree, it reduces prediction error. The following tree will repeat all the previous ones. Likewise, each tree will ultimately do likewise with all others. Each tree optimizes the differentiable loss function and reduces prediction error depending on its gradient. This strategy strengthens weak learning machines. We obtained the best result with a max tree depth of 6 and n-estimators of 45 trees after parameter adjustment. This method is fast, works with mixed-type data, handles missing data beautifully, doesn't change when input variables are changed monotonically and doesn't let input space outliers happen.

4.1.2. Distributed Random Forest (DRF)

Random Forest (Liaw and Wiener, 2002) classifies using ensemble machine learning. Like previously, it uses decision trees but builds a forest of random, uncorrelated trees to classify. Random replacement creates numerous training sets and trees. Randomly picking a subset of characteristics at each node splits the split in each tree. It prunes each tree to create random, uncorrelated trees. The model will then classify by averaging all three choices in the forest. Adding trees reduces volatility. This method manages large inputs and balances mistakes on imbalanced datasets (Fransiska Amalia Kurniawan, 2011). After parameter adjustment, a maximum tree depth of 20 and n-estimators of 38 trees in the decision-making forest yielded the best result.

4.1.3. Extreme Randomized Tree (XRT)

It generates several unpruned decision trees from the training database. Classification predictions are based on

majority votes. XRT splits somewhat randomly and does not repeat observations while forming a tree (Geurts *et al.*, 2006). The optimal split for XRT is also not used. In the algorithm, three hyper parameters are important: the number of decision trees in the ensemble, the number of input features that can be randomly selected and considered for each split point and the minimum number of samples needed for a node to form a new split point.

4.1.4. *Deep Learning (DL)*

Neural networks solve tough classification and regression problems. Feed forward neural networks start by adding input variables (features) with established labels. The interior layers use direction (training) and non-linear input and weights. There are numerous system-training algorithms. This study uses back-propagation. It has input, hidden, and output layers where a back propagation method optimizes perceptron unit weight. Back-propagation trains a multi-layered feed-forward neural network to reduce stochastic gradients. Prediction accuracy improves with adaptive learning rate, rate annealing, momentum training, drop-out, conventional L1 or L2 regularization, check pointing, and grid search (Hinton *et al.*, 2012). Data features can be automatically learned (Lecun *et al.*, 2015). Fig. 3. presents the model architecture.

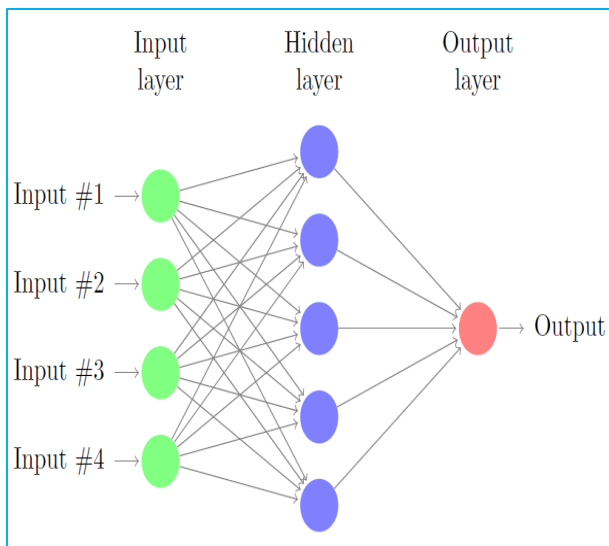


Fig. 3. The Architecture of a Deep Learning Algorithm (model).

4.1.5. *XGBoost*

XGBoost, a supervised learning technique, boosts models for accuracy. Boosting uses ensemble learning to build several sequential models in each new model to fix earlier model flaws.

4.1.6. *Generalized linear model (GLM)*

Assuming the prediction has a linear effect but not considering a specific distribution of exponential response variables improves the linear classification model.

4.1.7. *Stacked Ensemble (SE)*

Supervised ensemble machine-learning techniques use the best bagging, boosting and stacking prediction algorithms. Ensemble machine learning approaches produce greater predicted performance than any other learning algorithm by combining many algorithms. Popular machine learning techniques include ensemble learning (GBM, DRF). Bagging (DRF) and boosting (GBM) combine weak learners (decision trees) to create a strong learner. Stacking basic classifier predictions with a meta-learner creates an ensemble. A second-level “meta learner” is trained to determine the ideal combination of base learners in stacking algorithms, also known as super learning (Van Der Laan *et al.*, 2007) or stacked regression (Breiman, 1996). An ensemble approach combines the predictions of numerous base estimators to improve the robustness and generalizability of one predictor (Wolpert, 1992). This study proposes a stacked ensemble model including DRF, XRT, GBM, XGBoost, GLM and deep learning. This strategy trains a level 1 meta-model on out-of-fold predictions of base models (level 0) to forecast the ensemble model at level 1.

TABLE 3

Model contingency table for computation of Forecast quality

Fog (Visibility <1000 m), otherwise 0	Predicted (0)	Predicted (1)
Actual (0)	TN (True Negative)	FP (False Positives)
Actual (1)	FN (False Negative)	TP (True Positives)

4.2. *Statistical skill score analysis*

Table 3 shows the statistical skill score analysis utilizing a contingency table with logic: if fog (visibility <1000 m) then 1; otherwise 0; and if dense fog (visibility <200 m) then 1; otherwise 0. This analysis considers accuracy, precision, sensitivity, recall, hit rate, true positive rate, specificity, selectivity, and F1 score.

Overall accuracy measures classifier accuracy between 0 and 1. The number of correct guesses divided by all forecasts yields it. The most accurate is 1; the least accurate is 0.

$$Accuracy = \frac{(TP+TN)}{(TP+FP+FN+TP)} \tag{4}$$

Precision, or positive predictive value, measures how many positively predicted events are positive. It lies between 0 and 1.

$$Precision = \frac{(TP)}{(TP+FP)} \quad (5)$$

Recall, sensitivity, hit rate, or true positive rate measure the percentage of expected positives. Same as TPR. High sensitivity is 1, while low sensitivity is 0.

$$Recall = \frac{(TP)}{(TP+FN)} \quad (6)$$

To compute specificity, selectivity, or the correct negative rate, divide the number of valid negative predictions by the total number of negatives. The best specificity is 1, and the poorest is 0.

$$Specificity = \frac{(TN)}{(TN+FP)} \quad (7)$$

The F1 score represents the harmonic mean of precision and recall. It considers false positives and negatives. Thus, it excels on skewed datasets. It combines the model's precision and recall as the harmonic mean.

$$F_1 = \frac{2}{\frac{1}{recall} + \frac{1}{precision}} \quad (8)$$

4.3. Performance classification metrics

This study employed performance metrics: AUC measures how well the classification rule shown by the Receiver Operating Characteristic (ROC) curve works by combining the areas under the curve (Hand and Till, 2001). It aggregates performance across all categorization thresholds. Ranges from 0 to 1. False categorization is penalized by a log loss. Well-suited for multi-class categorization. Equation 9 represents the log loss for N samples from M. The log loss shows how well the predicted probability matches the actual value. Log loss increases when the expected probability varies from the real value.

$$Logarithmic\ loss\ or\ log\ loss = \frac{-1}{N} \sum_{i=1}^N \sum_{j=1}^M y_{ij} * \log(P_{ij}) \quad (9)$$

where, y_{ij} denotes the class of sample I.

The area under the precision-recall curve (AUCPR) is calculated for imbalanced datasets, it is better than the ROC curve since it measures accuracy and recall (sensitivity). Per-class mean error is for multi-class categorization only. It is a multi-class dataset's average class mistakes. This measure explains data misclassification across classes. Model performance

improves with lower metrics. The Gini index, or Gini impurity, is computed by subtracting the total of the squared probabilities of each class from one. It estimates the likelihood of randomly picked characteristics being misclassified. The categorization purity is 0 and it ranges from 0 to 1. 1 indicates random element distribution across classes, while 0.5 represents equal element distribution across select classes. The Gini coefficient measures how efficiently the predictor distinguishes parent node classes. Equation 10 represents it.

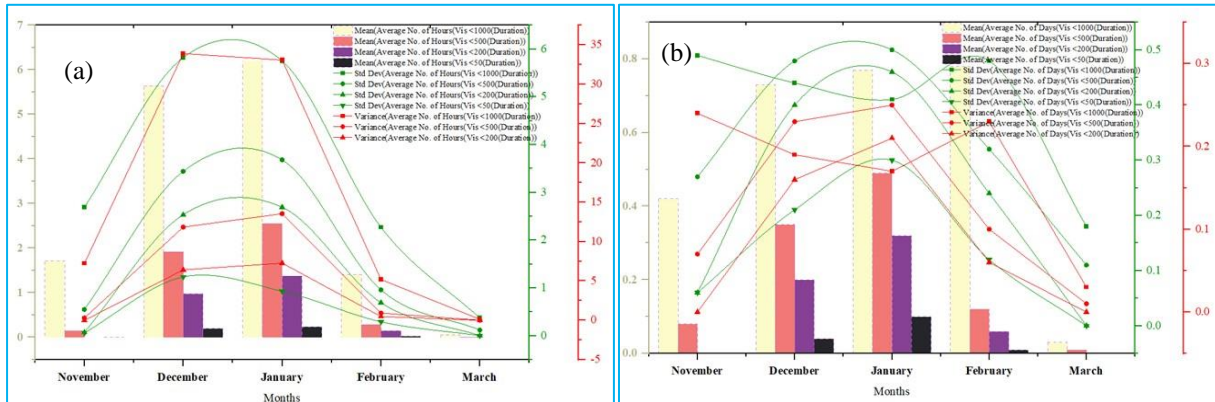
$$Ginni\ Index = \sum_{i=1}^C p(i) * (1 - P(i)) \quad (10)$$

5. Results and discussion

This section presents a statistical characterization of fog and dense fog, as well as a comparison of various ML approaches and the best-proposed algorithms tailored to Patna Airport for the short-range prediction of fog (visibility <1000 m) or dense fog (visibility <200 m). There were a total of 1210 days in the research period (from November 2014 to March 2022) with visibility below 1000 meters (fog) and 166 days with visibility below 200 meters (dense fog).

5.1. Statistical Characterization of Fog at Patna Airport

Figs. 4 (a) and (b) depict the statistical characterization of the duration of foggy weather, in hours and days, respectively, at Patna airport throughout the winter season, spanning from November to March. According to the data, there is a clear pattern to the occurrence of fog across all intensity levels, with January having the highest frequency and December and February coming in second and third. Conversely, the lowest frequency of fog is observed in the month of March. January experiences the longest period of fog, while March exhibits the shortest period of fog. Additionally, it can be observed that the frequency of foggy days, defined as those with visibility below 1000 meters, is similar. In the month of February, the occurrence of days with various levels of intensity is lower during this month. Additionally, the standard deviation indicates the variability observed in the months of November and February. Typically, fog of the radiation type is observed with high variability. However, during the months of January or occasionally in December, advection fog, especially in the rear sector of a western disturbance, occurs due to a higher standard deviation or lower variability. Regarding variability, the fog observed at Patna Airport has a regular pattern during the months of December and January. The elevated coefficients of variance during November and February, however, show a significant degree of unpredictability. The hours of intense



Figs. 4. (a&b). Statistical analysis of the number of fog (various intensity scales) (a) hours (b) days for November to March at JPNI Airport Patna, India.

TABLE 4

Mean number of hours of fog (visibility < 1000 m) and dense fog (visibility < 200 m) events (in hours) for the JPNI Airport, Patna

Months /Year		2014	2015	2016	2017	2018	2019	2020	2021	2022
November	Fog	5.33	2.96	0	0.7	0.6	2.4	0.06	1.06	--
	Dense fog	0	0	0	0	0	0.03	0	0	--
December	Fog	12.58	7.45	7.1	6.8	2.42	4.64	5.58	1	--
	Dense fog	2.71	0.74	0.5	0.285	0.03	0.77	1.06	0	--
January	Fog	--	5.87	7.67	10.25	12.83	3.61	6.25	7.16	5.58
	Dense fog	--	1.19	0.83	2.06	3.29	0.25	1.45	2.67	0.903
February	Fog	--	2.89	1.58	1.28	1.32	0.61	0.34	1.89	1.107
	Dense fog	--	0.035	0.31	0.28	0.178	0	0.103	0.178	0.285
March	Fog	--	0.16	0	0.03	0	0.09	0.16	0	0.16
	Dense fog	--	0	0	0	0	0	0	0	0

fog, characterized by visibility below 200 meters, exhibit a descending sequence of occurrences, with January having the highest frequency, followed by December and February. Similarly, when considering the number of days with dense fog, January surpasses both December and February. The average duration of fog hours (visibility <1000 m) and dense fog hours (visibility <200 m) throughout the period under investigation is displayed in Table 4.

5.2. Prediction of Fog (visibility <1000 m) using the ML approaches

This study aims to examine the classification results obtained from predicting fog (visibility <1000 m). Additionally, we provide a thorough assessment of the performance of several machine learning approaches on

these datasets. Which strategy demonstrated the highest level of effectiveness when applied to these datasets with a lead time ranging from 2 to 4 hours and so on? In this study, a total of seven machine-learning methodologies are employed to forecast the occurrence of fog. At level 0, the six base models-GBM, XGBoost, GLM, XRT, DRF, and deep learning-go through a process of trial and error to find the best performance by fine-tuning. At the level-1 evaluation stage, the suggested stacked ensemble of level-0 models does better than the six ML approaches at level 0. Table 5(a) illustrates the comparison of all seven machine learning methodologies for predicting fog (visibility <1000 m) for a lead time of 2 and 4 hours and Table 5(b) depicts the statistical skills cores of the proposed stacked ensemble modules for a lead time of 2 and 4 hours. In all the combinations and random selections of train and test datasets, stacked ensemble has superior

TABLE 5

(a) Performance metrics for the prediction of fog (visibility < 1000 m) for the lead times of 2 and 4 hours; (b) Statistical skill scores for the prediction of the proposed stacked ensemble models for the lead time of 2 and 4 hours

(a)	Types of Models	AUC		AUCPR		Gini Index		MPCE		Logloss	
		Lead Time		Lead Time		Lead Time		Lead Time		Lead Time	
		2	4	2	4	2	4	2	4	2	4
	GBM	0.905	AUC	0.879	0.863	0.809	0.779	0.165	0.170	0.480	0.432
	XGBoost	0.903	0.889	0.863	0.834	0.805	0.756	0.146	0.166	0.503	0.515
	DRF	0.931	0.878	0.912	0.867	0.863	0.808	0.156	0.143	0.393	0.407
	GLM	0.819	0.904	0.690	0.701	0.638	0.610	----	----	0.547	0.536
	XRT	0.903	0.805	0.863	0.819	0.806	0.742	0.160	0.157	0.442	0.483
	Deep Learning	0.924	0.871	0.913	0.903	0.847	0.831	0.143	0.142	0.357	0.389
	Stacked Ensemble	0.933	0.916	0.914	0.905	0.867	0.838	----	----	0.367	0.512

(b)	Proposed Models	Lead Time	Accuracy	Hit rate	Selectivity	Precision	Sensitivity	negative predictive Value	F1 Score
	Stacked Ensemble	2	0.85	0.85	0.83	0.89	0.85	0.79	0.87
		4	0.87	0.91	0.81	0.88	0.91	0.85	0.89

TABLE 6

(a) Performance metrics for predicting dense fog (visibility < 200 m) with two and four-hour lead times; (b) Statistical skill scores for predicting dense fog with the proposed stacked ensemble models with two and four-hour lead times

(a)	Types of Models	AUC		AUCPR		Gini Index		MPCE		Log loss	
		Lead Time		Lead Time		Lead Time		Lead Time		Lead Time	
		2	4	2	4	2	4	2	4	2	4
	GBM	0.972	0.918	0.918	0.806	0.943	0.837	0.089	0.103	0.910	0.302
	XGBoost	0.971	0.929	0.927	0.856	0.942	0.858	0.058	0.107	0.251	0.510
	DRF	0.966	0.933	0.884	0.823	0.932	0.867	0.071	0.103	0.214	0.396
	GLM	0.853	0.865	0.580	0.702	0.707	0.730	-----	-----	0.750	0.674
	XRT	0.967	0.913	0.912	0.779	0.933	0.827	0.065	0.116	0.211	0.317
	Deep Learning	0.912	0.893	0.813	0.774	0.823	0.787	0.145	0.160	0.422	0.517
	Stacked Ensemble	0.983	0.944	0.936	0.824	0.967	0.888	----	-----	0.248	0.51

(b)	Proposed Models	Lead Time	Accuracy	Hit rate	Selectivity	Precision	Sensitivity	Negative predictive value	F1 Score
	Stacked Ensemble	2	0.93	0.97	0.75	0.95	0.97	0.86	0.93
		4	0.92	0.96	0.75	0.95	0.96	0.80	0.92

performance compared to base models. The proposed stacked-ensemble models outperform all the base models at level 0, including deep learning neural networks. In a similar vein, the study conducts a comparison of performance metrics pertaining to lead durations ranging from 4 to 6 hours. The findings indicate that the suggested stacked ensemble models exhibit enhanced performance as the lead time diminishes. The empirical evidence indicates that when the time stamp decreases, there is an improvement in the AUC. The most favorable values for the prediction of fog fall within the range of 0.916 to 0.933 for the proposed stacked ensemble models.

5.3. Prediction of dense fog (visibility <200 m) by using machine learning

Table 6(a) presents a comprehensive analysis of the performance metrics of several ML approaches employed to forecast dense fog (visibility <200 m). Also, the statistical skill scores of the proposed stacked ensemble models are presented in Table 6(b). The evaluation is conducted using a test dataset, focusing on a lead time of 2 to 4 hours. The results show that stacked ensemble methods at level 1 perform better than the six base models at level 0, which is in line with the algorithms discussed in Section 4. The results have exhibited substantial improvement in comparison to the findings presented in subsection 5.2. All performance metrics and statistical skill scores show big improvements in predicting dense fog, which comes after fog for all lead times across all train and test dataset combinations. In terms of metric performance (shown in Table 6(a)), the stacked ensemble methods at level 1 have done better than level 0 machine learning approaches like GBM, XGBoost, GLM, XRT, DRF and deep learning. Additionally, proposed stacked ensemble methods have also exhibited higher statistical skill scores (illustrated in Table 6(b)). The accuracy of predictions within a lead time ranging from 4 hours to two hours exhibits variability, with values ranging from 92 % to 93%. The empirical evidence indicates that there is an improvement in the area under the receiver operating characteristic curve (AUC) as the time stamp decreases. The most favorable AUC values, ranging from 0.912 to 0.983, are seen for predicting dense fog. Moreover, the statistical skill score, such as the hit rate, exceeds 97%. The selectivity is greater than 75%, and the F1 score ranges from 0.92 (for a 4-hour advance time) to 0.93 (for a 2-hour lead time). These values indicate the effectiveness of the suggested models in predicting dense fog specifically for the Patna airport.

6. Discussion

Through historical data sets, this study looks at machine learning methods for predicting low visibility (fog or dense fog) in the nowcasting (02, 04 hours, *etc.*)

for airports. The recommended ensemble ML techniques at level 1 outperform the base models at level 0. F1 scores for fog predictions (visibility <1000 m) range from 0.87 to 0.89 (with a lead time of 4 to 2 hours). For dense fog (visibility <200 m), F1 scores vary from 0.92 (04 hours lead time) to 0.93 (02 hours lead time). This result backs up what (Van Der Velde *et al.*, 2010; Bergot and Koracin 2021; Castillo-Botón *et al.*, 2022) found: tree-based algorithms work very well (Dutta and Chaudhuri 2015; Bari and Ouagabi 2020). Except for a few authors, none others looked into these specific forecasts of fog in terms of the practical implications, *i.e.*, the robustness of the models that ensemble models will provide (Zhai and Chen 2018; Shankar and Sahana, 2023a). Low-visibility/fog forecasting is more difficult than wind speed, temperature, and precipitation forecasting. Despite this issue, any improvement in the explicit variance of poor visibility event prediction is vital for characterizing and accurately predicting these events and applying such predictive models in fog modelling (Shankar and Sahana, 2023b). Results from this experiment using ML algorithms lead to crucial findings.

(i) AUC increases with decreasing time stamps, with optimal values ranging from 0.916 to 0.9333 for fog (visibility <1000 m) and 0.944 to 0.983 for dense fog (visibility < 200 m) for 4 to 6 hours of lead time.

(ii) Our suggested techniques use an ensemble of multiple relevant ML algorithms (bagging, boosting, and stacking) to accurately forecast local-scale low visibility like fog (with an intensity scale), *etc.*

7. Conclusion

This study compares the performances of the base models at level 0, GBM, DRF, GLM, XRT, XGBoost and DL, with the proposed stacked ensemble models at level 1 for the nowcasting of the fog and dense fog. The proposed models optimize performance by choosing the optimum meta-algorithm trade-off (bagging, boosting and stacking) in the wide variety of proposed ML approaches. Additionally, while selecting the best prediction algorithms, ensemble models (level 1) integrate the base model information at level 0 to provide the optimum results in the nowcasting process of fog and dense fog. A comprehensive and wide analysis of ML approaches ensures the optimum outcome of the models and also ensures the robustness of the proposed models. The stacked ensemble approach (level 1) can forecast better than persistence and climatology; however, persistence delivers predictions with a short lead time. This forecasting method competes with human forecasts. This approach generates results for end-users like air traffic management and airline operators to extract their needs. Therefore, the proposed tailor-made nowcasting system

has the ability to optimize efficient traffic movement and the scheduling of the aircraft at the airport. Streamlining airport operations and flight scheduling will save money; hence, both the airport operator and airlines will utilize it. The proposed data-driven nowcasting method may be used at different airports; however, it must tune the ML models as per the local conditions. Also, large and diverse sets of data improve the ML models understanding of more complicated patterns and their ability to make accurate predictions of low visibility.

Acknowledgements

The authors appreciate the Director-General of Meteorology for his support and for providing facilities to carry out the study. Officials of Aerodrome Meteorological Office Patna are also thanked for their proposal and execution of the tailor-made nowcasting system for the optimum use of the resources in the winter 2023-2024.

Data Availability

The National Data Centre, Climate Research Station of the India Meteorological Department, provided hourly METAR data (or synoptic hourly data) of weather parameters at JPNI Airport Patna, which can be found at <https://dsp.imdpune.gov.in/>. Public access is available to this portal. Also, data can be supplied after a request.

Conflict of Interest

The authors declare no conflict of interest.

References

- Badarinath, K. V. S., Kharol, S. K., Sharma, A. R. and Roy, P. S., 2009, "Fog Over Indo-Gangetic Plains-A Study Using Multisatellite Data and Ground Observations", *IEEE J Sel Top Appl Earth Obs Remote Sens* **2**, 185-195. doi : <https://doi.org/10.1109/JSTARS>.
- Bari, D., Ouagabi, A., 2020, "Machine-learning regression applied to diagnose horizontal visibility from mesoscale NWP model forecasts", *SN Appl Sci*, **2**, doi : <https://doi.org/10.1007/s42452-020-2327-x>.
- Bartoková, I., Bott, A., Bartok, J. and Gera, M., 2015, "Fog Prediction for Road Traffic Safety in a Coastal Desert Region: Improvement of Nowcasting Skills by the Machine-Learning Approach", *Boundary-Layer Meteorol*, **157**, 501-516. doi : <https://doi.org/10.1007/s10546-015-0069-x>.
- Belo-Pereira, M. and Santos, J. A., 2016, "A persistent wintertime fog episode at Lisbon airport (Portugal): performance of ECMWF and AROME models", *Meteorol Appl* **23**, 353-370. doi : <https://doi.org/10.1002/met.1560>.
- Bergot, T., Koracin, D., 2021, "Observation, simulation and predictability of fog: Review and perspectives", *Atmosphere (Basel)*, **12**, 10-13. doi : <https://doi.org/10.3390/atmos12020235>.
- Boneh, T., Weymouth, G. T., Newham, P., Potts, R., Bally, A. E. and Korb, B. K., 2015, "Fog forecasting for Melbourne Airport using a Bayesian decision network", *Weather Forecast*, **30**, 1218-1233. doi : <https://doi.org/10.1175/WAF-D-15-0005.1>.
- Boudala, F. S., Isaac G. A., Crawford, R. W., Reid J., 2012, "Parameterization of runway visual range as a function of visibility: Implications for numerical weather prediction models". *J. Atmos Ocean Technol*, **29**, 177-191. doi : <https://doi.org/10.1175/JTECH-D-11-00021.1>
- Breiman, L., 1996, "Stacked regressions", *Mach Learn* **24**, 49-64. doi : <https://doi.org/10.1023/A:1018046112532>.
- Castillo-Botón C, Casillas-Pérez D, Casanova-Mateo C, Ghimire, S., Cerro-Prada, E., Gutierrez, P. A., Deo, R. C. and Salcedo-Sanz, S., 2022, "Machine learning regression and classification methods for fog events prediction", *Atmos Res* **272**. doi : <https://doi.org/10.1016/j.atmosres.2022.106157>
- Colabone, R. D. O., Ferrari A. L., Vecchia, FA. da S., 2015, "Tech ARB Application of artificial neural networks for fog forecast", *J Aerosp Technol Manag*, **7**, 240-246. doi : <https://doi.org/10.5028/jatm.v7i2.446>.
- Cornejo-Bueno L, Casanova-Mateo C, Sanz-Justo J, Cerro-Prada, E. and Salcedo-Sanz, S., 2017, "Efficient Prediction of Low-Visibility Events at Airports Using Machine-Learning Regression", *Boundary-Layer Meteorol* **165**, 349-370. doi : <https://doi.org/10.1007/s10546-017-0276-8>.
- Cornejo-Bueno S, Casillas-Pérez D, Cornejo-Bueno L, Chidean, I. M., Caamano, A. J., Sanz-Justo, J., Casanova-Mateo, C. and Salcedo-Sanz, S., 2020, "Persistence analysis and prediction of low-visibility events at valladolid airport, Spain", *Symmetry (Basel)*, **12**, 1-18. doi : <https://doi.org/10.3390/sym12061045>.
- Cornejo-Bueno S, Casillas-Pérez D, Cornejo-Bueno L, I, Chidean, M., Caamano, J. A., Elena Cerro-Prada, Carlos Casanova-Mateo and Sancho Salcedo-Sanz, 2021, "Statistical analysis and machine learning prediction of fog-caused low-visibility events at a-8 motor-road in spain", *Atmosphere (Basel)*, **12**, 1-22. doi : <https://doi.org/10.3390/atmos12060679>.
- Durán-Rosal AM, Fernández JC, Casanova-Mateo C, J. Sanz-Justo, S. Salced-Sanz and C. Hervás-Martínez, 2018, "Efficient fog prediction with multi-objective evolutionary neural networks", *Appl Soft Comput J*, **70**, 347-358. doi : <https://doi.org/10.1016/j.asoc.2018.05.035>.
- Dutta, D., Chaudhuri, S., 2015, "Nowcasting visibility during wintertime fog over the airport of a metropolis of India: decision tree algorithm and artificial neural network approach", *Nat Hazards* **75**, 1349-1368. doi : <https://doi.org/10.1007/s11069-014-1388-9>.
- Elith J, Leathwick JR and Hastie T., 2008, "A working guide to boosted regression trees", *J. Anim Ecol*, **77**, 802-813. doi : <https://doi.org/10.1111/j.1365-2656.2008.01390.x>.
- Fransiska, Amalia, Kurniawan, D., 2011, "Analisis dan Implementasi Random Forest dan Regression Tree (CART) Untuk Klasifikasi pada Misuse Intrusion Detection System", *Fak Tek Inform* 1-7.
- Geurts, P., Ernst, D. and Wehenkel, L., 2006, "Extremely randomized trees", *Mach Learn*, **63**, 3-42. doi : <https://doi.org/10.1007/s10994-006-6226-1>.
- Haefelin, M., Dupont JC, Boyouk N, Bayngardberm D., Laurent Gomes, Greg, Roberts and Thierry Elias, 2013, "A Comparative Study of Radiation Fog and Quasi-Fog Formation Processes During the ParisFog Field Experiment 2007", *Pure Appl Geophys*, **170**, 2283-2303. doi : <https://doi.org/10.1007/s00024-013-0672-z>.
- Hand, DJ, Till RJ, 2001, "A Simple Generalisation of the Area Under the ROC Curve for Multiple Class Classification Problems", *Mach Learn*, **45**,171-186. doi : <https://doi.org/10.1023/A:1010920819831>.

- Hinton, G. E., Srivastava N, Krizhevsky A, Sutskever, L., 2012, "Improving neural networks by preventing co-adaptation of feature detectors", 1-18.
- Hosea, M. K., 2019, "Effect of Climate Change on Airline Flights Operations At Nnamdi Azikiwe International Airport Abuja, Nigeria", *Sci. World. J.* **14**.
- IMD, Ministry of Earth Sciences G (2021) Standard Operation Procedure - Weather Forecasting and Warning Services Standard Operation Procedure Weather Forecasting and Warning
- Izett, J. G., van de Wiel B. J. H., Baas P., Hooft, A. V. and Schulte, R. B. and 2019 "Dutch fog: On the observed spatio-temporal variability of fog in the Netherlands", *Q. J. R. Meteorol Soc*, **145**, 2817-2834. doi : <https://doi.org/10.1002/qj.3597>.
- Jonnalagadda, J., Hashemi, M., 2020, "Forecasting Atmospheric Visibility Using Auto Regressive Recurrent Neural Network. In: Proceedings - 2020 IEEE 21st International Conference on Information Reuse and Integration for Data Science, IRI 2020", *Institute of Electrical and Electronics Engineers Inc.*, 209-215.
- Kneringer, P, Dietz S. J., Mayr, G. J. and Zeileis, A., 2019, "Probabilistic Nowcasting of Low-Visibility Procedure States at Vienna International Airport During Cold Season" *Pure Appl Geophys* **176**, 2165-2177. doi : <https://doi.org/10.1007/s000240181863-4>.
- Kutty, S. G., Agnihotri, G., Dimri, A. P., Gulpe, I., 2019, "Fog Occurrence and Associated Meteorological Factors Over Kempegowda International Airport, India", *Pure Appl Geophys* **176**, 2179-2190. doi : <https://doi.org/10.1007/s0002401818821>.
- La, I., Yum, S. S., Gulpe, I., Jae Min Yeom, Jae In Song and Joo Wan Cha, 2020, "Influence of quasi-periodic oscillation of atmospheric variables on radiation fog over a mountainous region of Korea", *Atmosphere (Basel)* **11**, doi : <https://doi.org/10.3390/atmos11030230>.
- Lecun, Y., Bengio Y., Hinton, G., 2015, "Deep learning", *Nature* **521**, 436-444. doi : <https://doi.org/10.1038/nature14539>.
- Liaw, A., Wiener, M., 2002, "Classification and Regression by random Forest", *R. News* **2**, 18-22.
- Mazoyer, M., Lac, C., Thouron, O., Bergot, T., Masson, V. and Musson-Genon, L., 2017, "Large eddy simulation of radiation fog: Impact of dynamics on the fog life cycle", *Atmos Chem Phys* **17**, 13017-13035. doi : <http://doi.org/10.5194/acp17130172017>.
- Miao, K. chao, Han T ting, Yao Y qing, Lu Hui, Peng Chen, Bing Wang and Jun Zhang, 2020, "Application of LSTM for short term fog forecasting based on meteorological elements", *Neurocomputing* **408**, 285-291. doi : <https://doi.org/10.1016/j.neucom.2019.12.129>.
- Mitsokapas, E., Schäfer, B., Harris, R. J., Beck, C., 2021, "Statistical characterization of airplane delays", *Sci Rep.* **11**, 1-11. doi : <https://doi.org/10.1038/s41598-021-87279-8>.
- Pahlavan, R., Moradi M., Tajbakhsh S and M. Rahnama, 2021, "Fog probabilistic forecasting using an ensemble prediction system at six airports in Iran for 10 fog events", *Meteorol Appl*, **28**, 1-16. doi : <https://doi.org/10.1002/met.2033>.
- Payra, S. and Mohan, M., 2014, "Multirule based diagnostic approach for the fog predictions using WRF modelling tool", *Adv Meteorol*, 2014, doi : <https://doi.org/10.1155/2014/456065>.
- Salcedo-Sanz, S., Piles, M., Cuadra, L., Casanova-Mateo, C., Caamano, A. J., Cerro-Prada, E. and Camps-Valls, G., 2021, "Long-term persistence, invariant time scales and on-off intermittency of fog events", *Atmos Res* **252**,. doi : <https://doi.org/10.1016/j.atmosres.2021.105456>.
- Sawaisarje, G. K., Khare, P., Shirke, C. Y., S. Deepakumar N. M. Narkhede, 2014, "Study of winter fog over Indian subcontinent: Climatological perspectives", *Mausam* **65**, 19-28. doi : <https://doi.org/10.54302/mausam.v65i1.858>.
- Shankar, A. and Giri, R. K., 2024, "The Impacts of Low Visibility on the Aviation Services of Patna Airport During the Period from 2016 to 2023", **3**.
- Shankar, A., Sahana, B. C., 2023a, "Early warning of low visibility using the ensembling of machine learning approaches for aviation services at Jay Prakash Narayan International (JPNI) Airport Patna", *SN Appl Sci.* doi : <https://doi.org/10.1007/s42452-023-05350-7>.
- Shankar A. and Sahana B. C., 2023b, "Efficient prediction of runway visual range by using a hybrid CNN-LSTM network architecture for aviation services", *Theor Appl Climatol.* doi : <https://doi.org/10.1007/s00704-023-04751-3>.
- Shatunova, M. V., Rivin, G. S. and Rozinkina, I. A., 2015, "Visibility forecasting for February 16–18, 2014 for the region of the Sochi-2014 Olympic Games using the high-resolution COSMO-Ru1 model", *Russ Meteorol Hydrol* **40**, 523-530. doi : <https://doi.org/10.3103/S106837391508004X>.
- Singh, A., George, J. P. and Iyengar, G. R., 2018, "Prediction of fog/visibility over India using NWP Model", *J Earth Syst Sci* **127**, 1-13. doi : <https://doi.org/10.1007/s12040-018-0927-2>.
- Steenefeld, G. J., Ronda, R. J. and Holtslag, A. A. M., 2015, "The Challenge of Forecasting the Onset and Development of Radiation Fog Using Mesoscale Atmospheric Models", *Boundary-Layer Meteorol* **154**, 265-289. doi : <https://doi.org/10.1007/s10546-014-9973-8>.
- Stolaki, S., Haefelin, M., Lac, C., Dupont, J. C., Elias, T. and Masson, V., 2015, "Influence of aerosols on the life cycle of a radiation fog event. A numerical and observational study", *Atm. Res.*, **151**, 146-161.
- Tyagi, S., Tiwari, S., Mishra, A., Singh, S., Hopke, P. K., Singh S. and Attri S. D., 2017, "Characteristics of absorbing aerosols during winter foggy period over the National Capital Region of Delhi: Impact of planetary boundary layer dynamics and solar radiation flux", *Atmos Res* **188**, 1-10. doi : <https://doi.org/10.1016/j.atmosres.2017.01.001>.
- Van, Der, Laan, M. J., Polley, E. C. and Hubbard, A. E., 2007, "Super learner", *Stat. Appl. Genet. Mol. Biol.*, **6**,. doi : <https://doi.org/10.2202/1544-6115.1309>.
- Van, Der, Velde, I. R., Steeneveld, G. J., Wichers, Schreur, B. G. J. and Holtslag, A. A. M., 2010, "Modeling and forecasting the onset and duration of severe radiation fog under frost conditions", *Mon. Weather Rev.* **138**, 4237-4253. doi : <https://doi.org/10.1175/2010MWR3427.1>.
- Wolpert, D., 1992, "Stacked Generalization (Stacking). Neural Networks **5**, 241-259.
- World Meteorological Organization, 2018, Guide to Instruments and Methods of Observation Volume I- Measurement of Meteorological Variables, 2018 editi. WMO-No. 8 © World Meteorological Organization, 2018, Geneva 2, Switzerland.
- World Meteorological Organization, 2019, Manual on Codes International Codes, 2019 editi. WMO-No. 306 © World Meteorological Organization, 2019.
- Zhai, B. and Chen, J., 2018, "Development of a stacked ensemble model for forecasting and analyzing daily average PM2.5 concentrations in Beijing, China", *Sci Total Environ*, **635**, 644-658. doi : <https://doi.org/10.1016/j.scitotenv.2018.04.040>.
- Zhu, L., Zhu, G., Han, L. and Wang, N., 2017, "The Application of Deep Learning in Airport Visibility Forecast", *Atmos Clim. Sci.* **07**, 314-322, doi : <https://doi.org/10.4236/acs.2017.73023>.